Available online at www.sciencedirect.com
ScienceDirect
European Journal of Pharmaceutics and Biopharmaceutics 69 (2008) 1083–1093
European Journal of Pharmaceutics and Biopharmaceutics
www.elsevier.com/locate/ejpb

Research Paper

Improved formulation of photosensitizer chlorin e6 polyvinylpyrrolidone for fluorescence diagnostic imaging and photodynamic therapy of human cancer

William Wei Lim Chin [a,b], Paul Wan Sia Heng [b], Patricia Soo Ping Thong [a], Ramaswamy Bhuvaneswari [a], Werner Hirt [c], Sebastian Kuenzel [c], Khee Chee Soo [a], Malini Olivo [a,b,*]

[a] *Division of Medical Sciences, National Cancer Centre Singapore, Singapore*
[b] *Department of Pharmacy, National University of Singapore, Singapore*
[c] *ORPEGEN Pharma, Heidelberg, Germany*

Received 18 November 2007; accepted in revised form 11 February 2008
Available online 10 March 2008

Abstract

An improved formulation of the photosensitizer chlorin e6 (Ce6) in combination with the hydrophilic polymer polyvinylpyrrolidone (PVP) was investigated for its potential clinical applications in fluorescence diagnosis and photodynamic therapy (PDT) of cancer. This study reports the comparative preclinical biodistribution and efficacy of Ce6 delivered with or without PVP versus dimethyl sulfoxide (DMSO). The safety and fluorescence pharmacokinetics of Ce6–PVP in humans was also accessed. Biodistribution results showed that Ce6–PVP had higher tumor to normal tissue ratio compared to the other formulations. The sensitivity and specificity derived from the area under the receiver operating characteristics curves showed that the formulations were able to discriminate tumor from peritumoral muscle in the following order: Ce6–PVP > Ce6 > Ce6–DMSO. In vitro PDT results showed that Ce6–PVP was found to induce selective phototoxicity in leukemic cells compared to peripheral mononuclear blood cells. In addition, in vivo light irradiation at 1 h after Ce6–PVP was found to induce greater tumor necrosis without causing animal toxicity. In patients, preferential accumulation of Ce6–PVP was observed in angiosarcoma lesions compared to normal skin following intravenous administration. In conclusion, PVP significantly enhanced the Ce6 concentration in tumors compared with Ce6 alone and increased the therapeutic index of PDT without any side effects in animal model. No serious adverse events were observed in human as well.

Keywords: Chlorin e6; Polyvinylpyrrolidone; Photosensitizer; Photodynamic therapy; Fluorescence diagnosis; Biodistribution; Imaging; Formulation

1. Introduction

Photodynamic therapy (PDT) is now well established as a clinical modality for the treatment of lung, esophagus, bladder, skin and head and neck cancers [1]. It involves the administration of a photosensitizer, followed by light irradiation in the presence of molecular oxygen in the target tissue. The combined action of these results in the formation of singlet oxygen, which is thought to be the main mediator of cellular death induced by PDT [2]. In addition, fluorescence diagnosis based on the accumulation of the

Abbreviations: Ce6, chlorin e6; PVP, polyvinylpyrrolidone; CCD, charge-coupled device; DMSO, dimethyl sulfoxide; EB, Evan's blue; PDT, photodynamic therapy; PBS, phosphate-buffered saline; ROS, reactive oxygen species; ROC, receiver operating characteristics.

* Corresponding author. Division of Medical Sciences, National Cancer Centre Singapore, 11 Hospital Drive, 169610 Singapore, Singapore. Tel.: +65 64368316; fax: +65 63720161.
E-mail address: dmsmcd@nccs.com.sg (M. Olivo).

0939-6411/$ - see front matter © 2008 Elsevier B.V. All rights reserved.
doi:10.1016/j.ejpb.2008.02.013

photosensitizer which emits fluorescence upon light excitation, is also emerging as a promising tool for the detection of small or poorly differentiated neoplastic changes [3].

Among the problems that are not yet adequately solved in the area of photosensitizer delivery are the difficulties in preparing pharmaceutical formulations that enable parenteral administration of the photosensitizer, poor tumoral selectivity, and a possible prolonged cutaneous photosensitivity due to slow elimination of the photosensitizer. Chlorins are promising photosensitizers with respect to their high phototoxic potential and relatively strong absorption in the red region of the visible spectrum leading to destruction of diseased tissue in deeper tissue layers. Although promising, chlorins are in general very lipophilic, making its administration in vivo relatively complicated. Water-soluble chlorin derivatives have been known to be prepared through stabilization and chemical transformation of lipophilic chlorophylls into a freely water-soluble sodium salt mixture. However, aqueous formulations or emulsions may not be suitable for tetra- or polypyrrole-based structures such as chlorins as these photosensitizers have an inherent tendency to aggregate by molecular stacking, which can severely curtail subsequent photosensitization processes [4,5]. Therefore, multiple means of delivering chlorin-based photosensitizers have been explored ranging from liposomal formulation, glycoconjugation, microspheres, entrapment in biodegradable nanoparticles, to the use of excipients such as dimethyl sulfoxide (DMSO). Due to its amphiphilic nature of DMSO, it is used frequently to dissolve chemicals with poor water solubility. But the toxicological consequence of its interaction with a photosensitizer still remains unclear. Biocompatible block copolymers are also used increasingly in the pharmaceutical industry to enhance drug solubility and bioavailability [6]. Polymer–photosensitizer conjugation or encapsulation of the photosensitizer in colloidal carriers such as oil-dispersions, liposomes and polymeric particles has been investigated [7,8]. Polymers currently being used with chlorin derivatives are polyethyleneglycol and *N*-(2-hydroxypropyl) methacrylamide (HPMA) [9–11].

In our pursuit for strategies to optimize the photosensitizer chlorin e6 (Ce6) for improved fluorescence diagnosis and photodynamic therapy of cancer, we have investigated the formulation of Ce6 with polyvinylpryrrolidone (PVP). Ce6 has improved efficacy and has decreased side effects compared to first generation photosensitizers from hematoporphyrin derivatives. PVP is nontoxic, biocompatible, generally recognized as safe, and is a widely used soluble additive in the pharmaceutical area. PVP is known to form water-soluble complexes with a number of pharmacological substances and investigations into the formation of PVP-complexes with drugs have been described [12,13]. This pharmaceutical formulation was developed with the rationale to provide a novel photosensitizer with a high photochemical stability, good solubility both in water and in biological fluids, high affinity to the target tissue, large depth of necrosis, efficient generation of the active species that cause destruction of the pathologically changed tissue, low phototoxicity in normal tissue as well as to provide a method of preparation of such photosensitizer. In our previous studies, we have reported the potential application of Ce6–PVP in the fluorescence diagnosis and photodynamic therapy of human nasopharyngeal and bladder carcinomas in preclinical models [14–17] and in one angiosarcoma patient [18]. The purity of Ce6 in this formulation contained not less than 75% with the remaining composition consisting of purpurins [19].

In this report, we further investigated the uptake and photodynamic activity of the newly improved formulation of Ce6–PVP. The weight ratio of the sodium salt of Ce6 and PVP remained at 1:1 and the purity level of Ce6 was optimized to 92–99%. Recently, we have reported the efficacy of this new Ce6–PVP formulation for fluorescence diagnosis and PDT of small cell lung carcinoma and non-small cell lung carcinoma [20]. We now present the comparison of in vitro photocytotoxicity data on leukemic cells and peripheral mononuclear blood (normal) cells using Ce6 and Ce6–PVP. We compared the sensitivity and specificity of temporal fluorescence intensities of Ce6, Ce6–PVP and Ce6 delivered using DMSO in normal tissue versus tumor tissue as well as the biodistribution in various organs. PDT was also performed to compare the efficiency in inducing tumor necrosis of the human bladder carcinoma xenografts. This study also examines the fluorescence distribution of Ce6–PVP in angiosarcoma lesions and normal skin in patients.

2. Methods

2.1. Photosensitizers and chemicals

The original Ce6–PVP also known as Fotolon or Photolon (hereafter designated as 75% Ce6–PVP) preparation was prepared at RUE Belmedpreparaty, Minsk, Belarus [21]. The new formulation of Ce6–PVP manufactured by ORPEGEN Pharma GmbH, Heidelberg, Germany was relatively free of impurities, and the purity of the drug is around 92–99%. In both cases it was a co-lyophilisate of Ce6 sodium salt and PVP (pharmaceutically grade polymer, molecular mass $\approx$ 12,000 g/mol) in a 1:1 mass ratio. Ce6 sodium salt lyophilized without further addition of PVP and is readily soluble in aqueous solution. An alternate source of Ce6 in the acetic acid form was obtained from Frontier Scientific (Logan, Utah). It was dissolved in dimethyl sulfoxide (DMSO) (Sigma, USA) to give a 1 mM stock solution; and diluted further with 0.9% sodium chloride (NaCl) to constitute a 10% DMSO concentration in the final preparation immediately before intravenous adminstration.

2.2. In vitro photosensitizing efficacy

To distinguish between necrotic and apoptotic cells following PDT, Annexin V binding and propidium iodide (PI) uptake were assessed by flow cytometry using a commer-

cially available kit according to the instructions by the manufacturer. Peripheral mononuclear blood (PMN) cells obtained from healthy volunteers and a K562 leukemic cell line were used for this experiment. Cells were incubated with 10 μM of either Ce6 or Ce6–PVP for 30 min before exposure to a light dose of 1 J/cm^2. Cells were harvested and resuspended in binding buffer provided in the kit. Designated concentration of the Annexin V stock solution and PI stock solution were added to the cell suspension. After incubation for 10 min in the dark, the cells were immediately analyzed with a FACScan flow cytometer (Becton Dickinson) equipped with an excitation laser line at 488 nm. The FITC – Annexin V (green fluorescence) and the PI (orange fluorescence) were collected in log scale through 530 ± 20 and 575 ± 15 nm band pass filter, respectively.

2.3. Animal model

Male Balb/c athymic nude mice, 6–8 weeks of age, weighing an average of 24 g were obtained from the Animal Resource Centre, Western Australia. MGH, poorly differentiated human bladder carcinoma cells were used to induce subcutaneous tumor xenografts. The cells were cultured as a monolayer in RPMI-1640 medium supplemented with 10% fetal bovine serum, 1% non-essential amino acids (Gibco, USA), 1% sodium pyruvate (Gibco, USA), 100 units mL^{-1} penicillin–streptomycin (Gibco, USA) and incubated at 37 °C, 95% humidity and 5% CO_2. Before inoculation, the cell layer was washed with phosphate-buffered saline (PBS), trypsinized, and counted using a hemocytometer. Approximately 3.0×10^6 MGH cells suspended in 150 μl of Hanks' Balanced Salt Solution (Gibco, USA) were subcutaneously injected into the lower flanks of the mice. The animals were used for experiments when the tumors measured around 7–10 mm in diameter. This ensured that the tumor sizes was kept consistent to minimize variations due to the degree of vascularization of the implants. All procedures were approved by the Institutional Animal Care and Use Committee, SingHealth, Singapore, in accordance with international standards.

2.4. Fluorescence imaging and image analysis

Mice were randomly assigned to receive a dose of 2.5 mg/kg of the Ce6–PVP, Ce6 or Ce6–DMSO via tail vein injection. At 0, 1, 3 and 6 h post-drug administration, mice were sacrificed and the skin overlaying the tumor was carefully removed to expose the tumor and normal peritumoral muscle for fluorescence imaging. A commercially available fluorescence endoscopic system (Karl Storz, Tuttlingen, Germany) was used to perform the macroscopic fluorescence digital imaging. A modified xenon short arc lamp (D – Light system in blue light mode, Karl Storz) filtered by a band pass filter (375–480 nm) was used for the excitation of the photosensitizer in tissue. Fluorescence was captured via a sensitive CCD camera (Tricam SL PAL, Karl Storz) attached to an endoscope integrated with a long pass filter (cut-off wavelength 560 nm). The red channel registered the photosensitizer fluorescence and the blue channel captured the diffusely back-scattered excitation light. The distance between tissue surface and probe lens was standardized before imaging. This was done to minimize variations due to geometrical factors such as fluorescence excitation and collection angles. In addition, a short exposure of the surface of tumor and peritumoral muscle to the excitation light (10 s) was performed to avoid excessive photobleaching effects. The intensities of the red (IR) and blue channels (IB) of the fluorescence images were extracted using the software MicroImage (Olympus Optical Co. (Europa) GmbH, Germany) according to the following equation:

$$\mathrm{IR_N} = [\mathrm{IR}_t/\mathrm{IB}_t] - [\mathrm{IR}_{t0}/\mathrm{IB}_{t0}] \quad \text{(equimolar dose of Ce6 administered)} \tag{1}$$

with $\mathrm{IR_N}$ = normalized relative fluorescence intensity of tumor or peritumoral muscle at time, t, after drug administration; IR = intensity of red channel; IB = intensity of blue channel; t = time in hours after drug administration; t_0 = time before photosensitizer administration. The red-to-blue intensity ratio algorithm is independent of the observation geometry, the distance between the endoscope tip and the observed tissue as well as the fluctuation of the excitation irradiance [22].

2.5. Nonlinear regression and statistical analysis of fluorescence intensity

The normalized relative fluorescence intensities (after substraction of background signal of fluorescence intensities) versus time obtained from Eq. (1) were analyzed by means of nonlinear regression method (Graph-Pad Prism™ Version 4.03) by fitting a three parameter mono-exponential decay curve to fit the K, decay rate constant (in h^{-1}). Bi-exponential decay curves fit the data more poorly than the mono-exponential ones and were therefore not considered for the analysis. The validity of K in the mono-exponential model was verified with the test of runs in each case. For all of the fits, the test of runs did not detect any deviation from the model of monoexponential decay. To compare the fits of the Ce6 formulations to each data set, the K was compared using extra sum-of-squares F test by comparing a global fit (one shared best-fit K value for all the data sets) to individual fits (a different best-fit K value for each data set). For all the formulations, the F tests showed that the individual fits for tumor, peritumoral muscle and skin were determined as the preferred fit in the analysis. These ratios for tumor and peritumoral muscle from 1 to 6 h post-drug administration were then analyzed for sensitivity and specificity in demarcating tumor from peritumoral muscle by fitting the data into the receiver operating characteristic (ROC) curve (Graph-Pad Prism™ Version 4.03). The ROC curve illustrates the tradeoff between sensitivity and specificity by plotting the tumor fluorescence against the peritumoral fluorescence

for the different possible probability thresholds of a fluorescence diagnostic test of the various Ce6 formulations. White light imaging was used to confirm the presence of tumor and peritumoral muscle.

2.6. Chemical extraction and spectrofluorimetry analysis

After imaging at 1, 3 and 6 h, the following tissues were removed and rinsed with PBS: tumor, muscle, skin, liver, spleen, kidney, brain, heart, lung, large intestine and small intestine. The organs were then blotted dry on tissue paper, weighed and frozen at −80 °C until extraction. Samples of each tissue (15–35 mg) were mixed with 1–2 mL of Solvable™ (Packard Instrument, USA) and incubated at 50 °C for 16 h in the dark as described previously by Bellnier et al. [23]. Solvable™ contains 3% *N*,*N*-dimethyl lauryl amine oxide, 3% alkyloxypolyethyleneoxyethanol and 2% sodium hydroxide in water. We have confirmed that this method did not affect the fluorescence property of Ce6 (unpublished data). The fluorescence ($\lambda_{em} = 665$ nm) of the solubilized samples was measured by a spectrofluorophotometer (model RF-5301 PC, Shimadzu; $\lambda_{ex} = 400$ nm). The level of fluorescence intensity of the tissue samples is proportional to the tissue concentration of Ce6. The background fluorescence before drug administration was also subtracted and was normalized to the weight of organs. Dunn's multiple comparison test was performed on the various groups. Statistical significance was accepted at $p < 0.05$

2.7. PDT treatment on murine xenograft model

A dose of 5 mg/kg of the photosensitizer was administered intravenously through the tail vein. The mice were anaesthetized with 80–100 μl of a cocktail of ketamine hydrochloride (50 mg/ml, Trittau, Germany) and valium (1:1 vol/vol) through intraperitoneal injection. A portable diode laser (Ceralas PDT 665, Biolitec) emitting at a wavelength of 668 ± 3 nm was used for irradiation. The peak power output was calibrated to 1.65 W at the fiber tip before commencement of irradiation. The laser energy with a total fluence of 100 J/cm^2 was delivered to the surface of the tumor via a silica fiber frontal light distributor (FD model, Medlight, Switzerland). The fiber was positioned to produce a 1.0 cm^2 circular spot of light irradiation. A fluence rate of 83 mW/cm^2 was measured using a power meter (LaserCheck, Coherent, USA). PDT treatment was performed after a drug–light interval (DLI) of either 1 or 3 h on anaesthetized mice.

2.8. Assessment of tumor response post-PDT

The evaluation of tumor cell death was performed using Evans Blue (EB) (Merck, Germany) vital staining. At 48 h post-PDT, 1% EB in PBS was injected intraperitoneally at a volume of 0.4 mL. Six hours later, mice were sacrificed and the tumors were excised. Then, around 2–3 mm thick cross-section slices were cut and imaged under a stereoscopic microscope (Stemi 2000C, Zeiss, Germany). The unstained area was attributed to tissue cell death, whereas the stained area indicated viable tissue. Digital images were saved in JPEG format, and all analyses were carried out using NIH ImageJ 1.37v software. Each image captured had the same calibration values to allow uniformity in the processing of the images. The tumor was outlined using the freehand drawing tool to measure the total tumor area. Similarly the necrotic area of the tumor was measured. The percentage of tumor cell death was calculated as the necrotic area divided by the total tumor area multiplied by 100.

2.9. Clinical study

The clinical study was approved by the Clinical Ethics Committee, National Cancer Centre Singapore. Fluorescence imaging was performed on 3 patients with histologically confirmed angiosarcoma that underwent PDT. All were male with a median age of 61 years. Patients were intravenously administered with 2–4 mg/kg of 75% Ce6–PVP prepared in 0.9% NaCl. The solution was intravenously injected over 10 min of infusion. Fluorescence imaging was performed on various parts of the lesion and normal skin from 1–3 h post-drug administration (before PDT) and 5, 6 and 48 h post-drug administration (post-PDT). Fluorescence intensities were tabulated as follows:

$$I_{Nt} = IR_t/IB_t \quad (3)$$

with I_{Nt} = normalized fluorescence intensity after time, t; IR = intensity of red channel; IB = intensity of blue channel; t = time in hours after drug administration. All patients had to remain in minimum ambient light for 48 h.

3. Results

3.1. In vitro photosensitizing efficacy

Ce6–PVP and Ce6 were evaluated for their photocytotoxicity against K562 leukemic cell line and peripheral mononuclear cells (Fig. 1). Necrotic cells were identified through PI staining and apoptotic cells were identified through Annexin V staining, detected by flow cytometry after PDT. Cells illuminated without the photosensitizers and cells kept in the dark in the presence of the photosensitizers did not present any significant loss of viability. For the K562 cell line, total dead cells were estimated to be around 90% and 100% for Ce6–PVP and Ce6, respectively. On the contrary, under the same treatment condition, the peripheral mononuclear blood cells treated with Ce6–PVP exhibited relatively lower percentage of total dead cells (70%, $p < 0.01$) compared to Ce6 (90%).

3.2. Biodistribution of Ce6 formulations

The amount of photosensitizers from tumor, peritumoral muscle and skin was quantified using the chemical fluorescence extraction technique and cuvette-based spectrofluori-

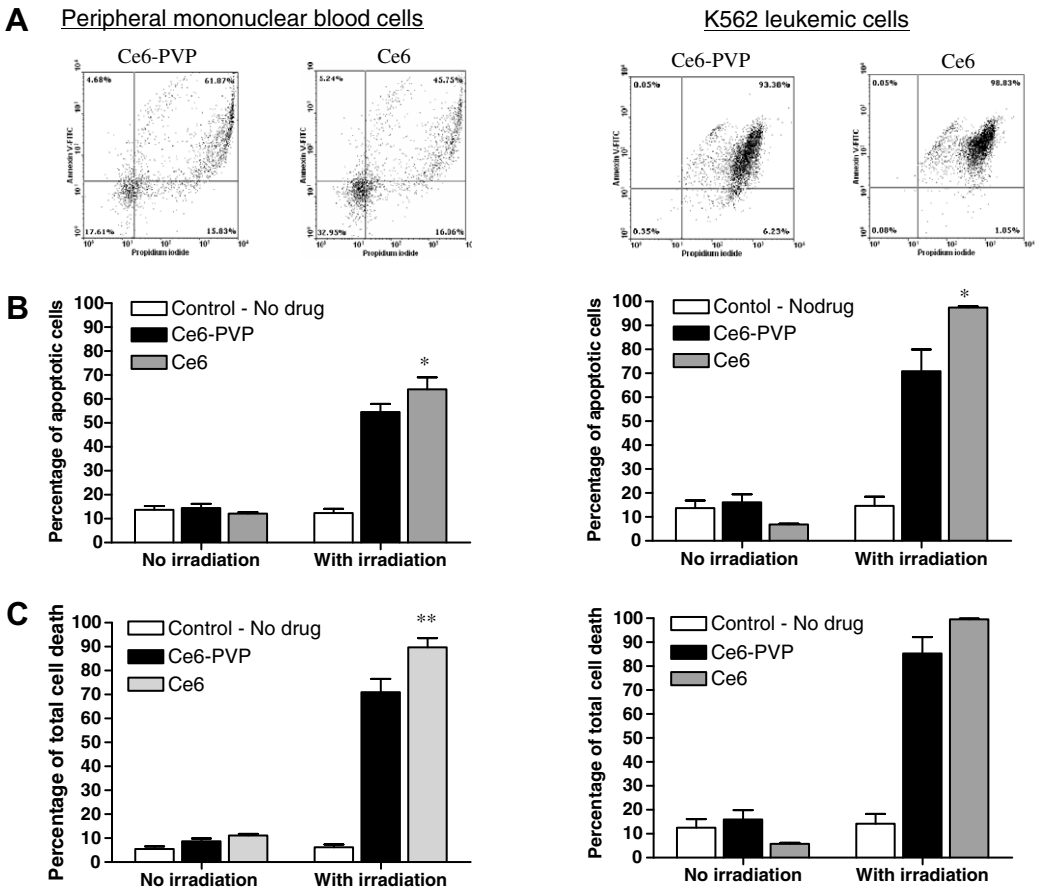

Fig. 1. (A) Representative of flow cytometry analysis of PDT induced apoptosis and necrosis for PMN blood (normal) cells (left panel) and K562 leukemic cells (right panel) after treatment with Ce6 and Ce6–PVP. Induction of apoptosis and necrosis, was detected through the accumulation of Annexin-V and propidium iodide (PI) stained cells, respectively. Cells were incubated with a concentration of 10 μM of either Ce6 or Ce6–PVP for 30 min before light irradiation of 1 J/cm^2. Three main subpopulations, corresponding to viable cells (lower left quadrant), apoptotic cells stained with Annexin-V (upper right quadrant), and dead/necrotic PI-stained cells (lower right quadrant), can be readily differentiated. (B) In terms of apoptosis, both Ce6 and Ce6–PVP demonstrated lower percentage of apoptotic cell death in PMN cells compared to K562 leukemic cells. However, Ce6 displayed higher photocytotoxicity in both PMN and K562 cells compared to Ce6–PVP, indicating the potency of Ce6. (C) When the total percentage of cell death (apoptosis and necrosis) was tabulated, Ce6 was found to induce significant cell death in PMN cells compared to Ce6–PVP, indicating toxicity to normal cells, while for K562 cells photocytotoxicity was comparable between the Ce6 and Ce6–PVP. For K562 cells, data for Ce6–PVP represent a mean value of 6 replicates while data for Ce6 represent a mean value of three replicates. For PMN cells, data for Ce6–PVP represent a mean value of 15 replicates taken from five volunteers while data for Ce6 represents a mean value of six replicates taken from two volunteers. Bars = SD. Statistical significance was calculated by two-way ANOVA with Bonferroni post-hoc test ($^{*}p < 0.05$ and $^{**}p < 0.01$ with respect to Ce6–PVP).

metry (Fig. 2). The amount of Ce6–PVP accumulation was significantly higher in the tumor, muscle and skin in comparison to Ce6 at all time points. Ce6–DMSO tumor accumulation was observed to increase 24-fold compared to Ce6 at 1 h. Similarly, Ce6–DMSO accumulation was higher in muscle and skin at 3 and 6 h post-administration compared to Ce6. The tumor to normal peritumoral muscle ratio for Ce6–PVP was higher compared to Ce6 (Table 1) suggesting that Ce6–PVP has a good tumor tissues accumulation ratio, with no significant accumulation in other normal tissue. Although Ce6–DMSO showed the highest tumor to normal peritumoral muscle ratio, it also resulted in higher accumulation in other normal organs (Fig. 3 and Table 1). Fig. 3 shows comparative biodistribution of Ce6–PVP, Ce6 and Ce6–DMSO in eight organs using chemical extraction method. The data demonstrates that the amount of drug was comparable in all the organs between Ce6 and Ce6–PVP. In contrast, the amount of the Ce6–DMSO accumulation was significantly 10-fold higher in the liver, spleen, kidney, brain, heart and lung. The most significant amount of photosensitizer detected from all of the tested formulations was concentrated in the small and large intestines with relatively similar concentrations. The accumulation of Ce6–PVP in tumor significantly exceeded liver, spleen, kidney, brain, and heart tissues compared to Ce6.

3.3. Sensitivity and specificity of Ce6 formulations

Fig. 4 displays a ROC curve that illustrates the ability of Ce6, Ce6–PVP and Ce6–DMSO induced fluorescence to discriminate between tumors and peritumoral muscle. Area under the ROC curve was used to compare the sensitivity

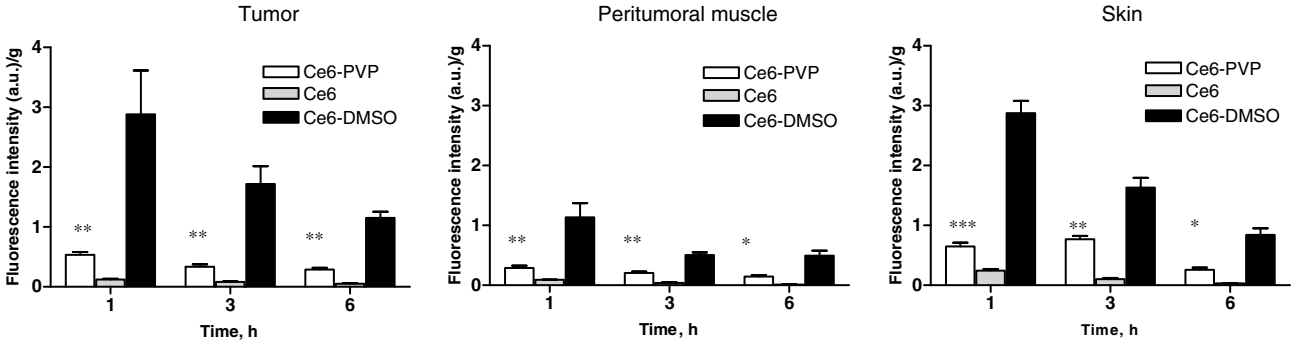

Fig. 2. Comparison of biodistribution of Ce6–PVP, Ce6 and Ce6–DMSO in tumor, muscle and skin at 1, 3 and 6 h post-drug administration, respectively, using chemical extraction method. For all data points, $n = 4 \pm$ SD. Statistical significance was calculated by two-way ANOVA with Bonferroni post-hoc test ($^{*}p < 0.05$; $^{**}p < 0.01$, $^{***}p < 0.001$ with respect to Ce6). All Ce6–DMSO data points were statistically significant with respect to Ce6.

Table 1
Comparison of tumor to normal tissue ratio in various organs after intravenous administration of 5 mg/kg Ce6–PVP, Ce6 or Ce6–DMSO

	Muscle	Skin	Liver	Spleen	Kidney	Brain	Heart	Lung
Ce6–PVP	1.8	1.5	2.0	23.5	10.1	16.6	15.5	2.9
Ce6	1.0	0.4	1.2	2.9	3.0	3.9	3.1	4.3
Ce6–DMSO	2.6	1.0	1.2	8.5	15.6	0.9	3.1	5.9

[a]Ratio was calculated by dividing the fluorescence intensity span of tumor to the fluorescence intensity span of the various tissues from 1 to 6 h post-drug administration. The span was tabulated using nonlinear regression analysis.

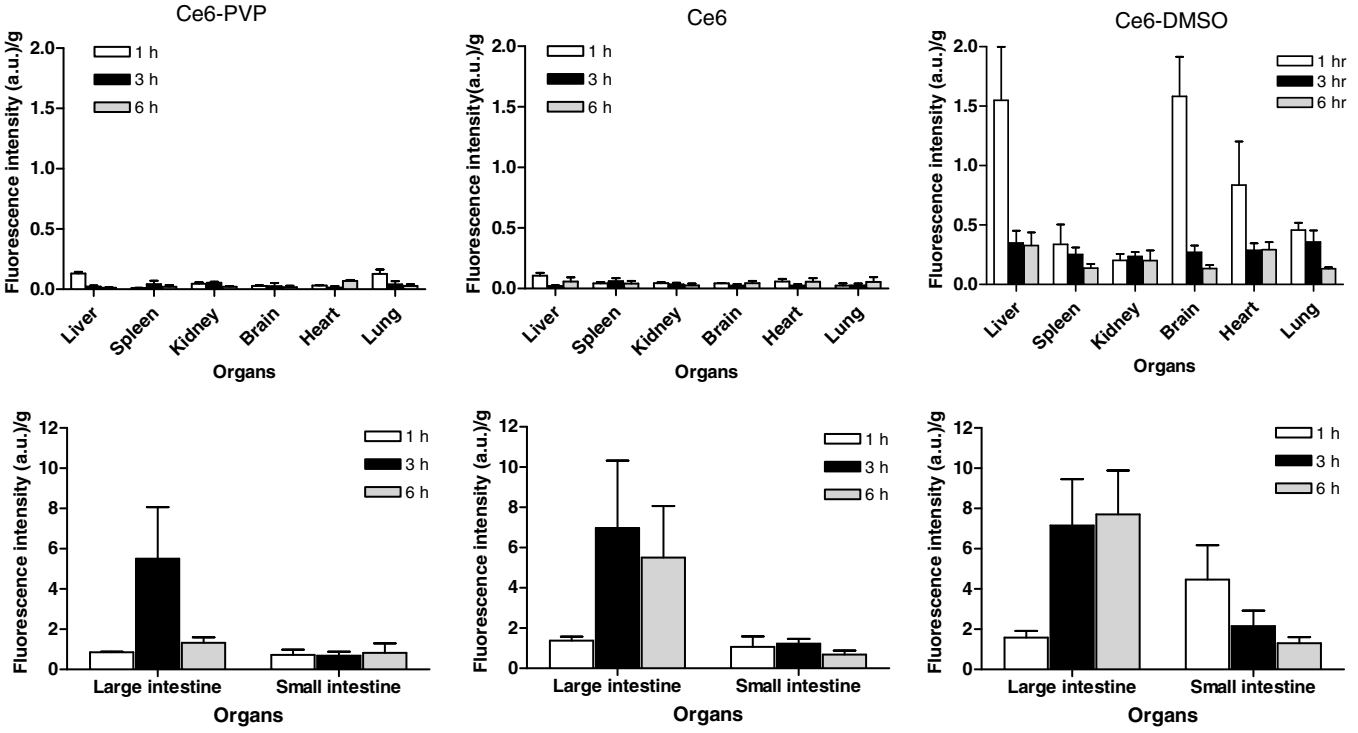

Fig. 3. Comparison of biodistribution of Ce6–PVP, Ce6 and Ce6–DMSO in normal tissue of various organs in mice using chemical extraction method. Each data point represents a mean of 3 animals ± SD.

and specificity of the temporal fluorescence of the three formulations. A non-discriminative fluorescence has an area of 0.5. A perfect discriminative fluorescence has an area of 1.00. The area under the ROC curve was 0.98 ± 0.02 for Ce6–PVP ($p = 0.0001$), 0.95 ± 0.05 for Ce6 ($p = 0.003$) and 0.83 ± 0.1 ($p = 0.0246$) for Ce6–DMSO. The optimal cut-off level of fluorescence intensity that maximizes 100% sensitivity for Ce6–PVP yielded 83% specificity, but a lower specificity of 73% and 58% for Ce6 and Ce6–DMSO, respectively. To further evaluate the effect

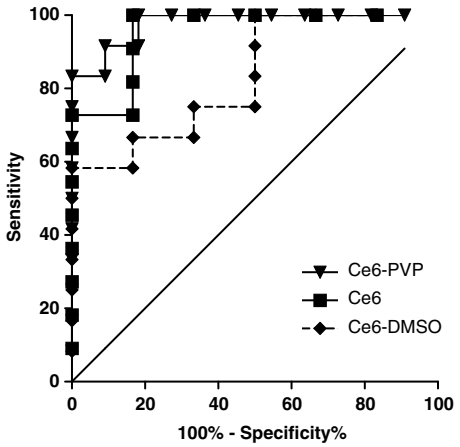

Fig. 4. ROC curves comparing fluorescence intensities of Ce6–PVP, Ce6 and Ce6–DMSO for classifying tumor from peritumoral muscle. The areas under the curve (AUC) were then compared in order to make a fair judgment of the effectiveness of Ce6 formulations without being constricted to single values of sensitivity and specificity, which largely depend on the cut-off fluorescence intensity value chosen to distinguish normal from malignant tissue. The closer the curve comes to the 45-deg diagonal solid line, the less accurate the fluorescence diagnostic. The following is a rough guide for classifying the accuracy of fluorescence intensities based on the AUC: 1–0.9 = excellent; 0.9–0.8 = good; 0.8–0.7 = fair; 0.7–0.6 = poor; and 0.6–0.5 = fail. The AUC for Ce6–PVP, Ce6 and Ce6–DMSO were 0.98 ± 0.02, 0.95 ± 0.05 and 0.83 ± 0.1, respectively. The ROC curves also potentially demonstrate how the fluorescence diagnostic scheme can be adjusted to obtain the desired degree of sensitivity at the cost of specificity. Ce6–PVP induced fluorescence showed the highest sensitivity and specificity in detecting tumor from peritumoral muscle.

of PVP on the retention rate of Ce6 fluorescence in comparison to Ce6 alone or Ce6 delivered using DMSO, the decay rate constant (K) of the photosensitizer fluorescence in tumor tissues has been estimated from 1 to 6 h post-drug administration. Fluorescence intensity of Ce6–PVP ($K = 0.1386 \pm 0.04\ h^{-1}$) was retained longer in tumor compared to Ce6 ($0.1755 \pm 0.04\ h^{-1}$) and Ce6–DMSO ($0.2007 \pm 0.08\ h^{-1}$). As such, the half-life was calculated to be 5.0, 3.9 and 3.4 h for Ce6–PVP, Ce6 and Ce6–DMSO, respectively.

3.4. In vivo photodynamic therapy on tumor xenografts

The extent of tumor necrosis was identified using vital staining with EB at 48 h post-PDT (Fig. 5). The results of these experiments are presented in Table 2. Complete tumor necrosis was achieved when irradiation was performed at 1 h drug–light interval using Ce6–PVP. At 3 h drug–light interval, Ce6–PVP-treated tumors exhibited $40 \pm 9.8\%$ necrosis. No adverse side effects were observed in any animal at post-PDT after the administration of Ce6–PVP. At the same drug and light dose, complete tumor necrosis was observed for only 67% of Ce6-treated animals at 3 h drug–light interval. Severe side effects were observed for animals treated at 1 h drug–light interval post-Ce6 administration and animals treated at 1 and 3 h post-Ce6–DMSO administration.

3.5. Fluorescence imaging of angiosarcoma lesions

Patients with angiosarcoma were given 2–4 mg/kg of 75% Ce6–PVP through intravenous administration. No side effects or complications were observed during or after intravenous drug administration, other than transient pain at the lesion sites during PDT. The clinical outcome for one patient is noteworthy, with distinct untreated lesions spontaneously regressing following PDT of selected lesions as reported [18]. We hypothesized that this could be due to a PDT-activated immune response. The photosensitizer accumulation in tissue can be visualized through its typical red fluorescence after blue light excitation (Fig. 6). Clear demarcation of the lesion was observed in the fluorescence image indicating excellent selectivity of the photosensitizer. Fluorescence in the lesion was more intense compared to the fluorescence in the normal skin. The intensity in the lesions increased rapidly over the first 3 h to reach maximum intensity (Fig. 7). At the 5th hour, immediately after PDT, 75% Ce6–PVP fluorescence was found to decrease in the tumor (tumor to normal ratio = 1.9). At 48 h, the overal fluorescence was lower but still sustained in the lesions. Fluorescence intensity was low at all times in the normal skin compared to the lesions.

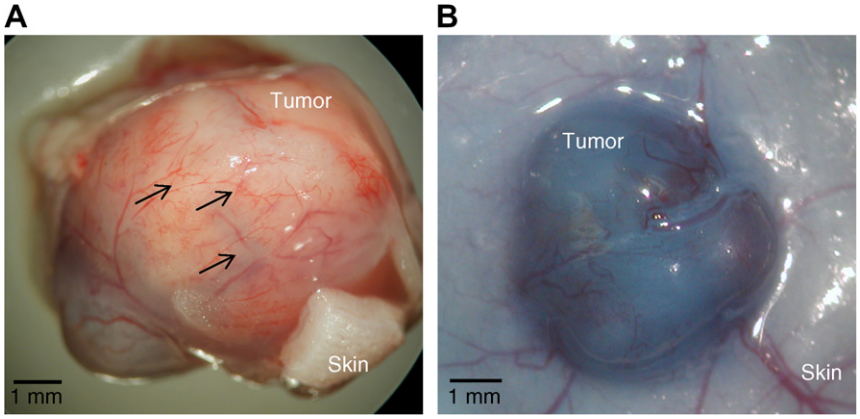

Fig. 5. A representative macroscopic view of whole MGH tumor xenograft stained with Evans Blue dye at 48 h post-PDT after treatment at 1 h drug–light interval mediated PDT with Ce6–PVP (A) and control tumor (with Ce6–PVP, no light irradiation) (B). Necrotic tumor tissue appeared white and was almost devoid of vital staining. Shrinkage of tumor blood vessels was observed on the surface of tumor (arrow).

Table 2
A comparison of the percentage of necrotic tumor and survival of mice evaluated at 48 h post-PDT after the administration of 5 mg/kg Ce6–PVP, Ce6 or Ce6–DMSO with irradiation at a fluence and fluence rate of 100 J/cm^2 and 85 mW/cm^2, respectively

Photosensitizer	Percentage of necrotic tumor tissue (%) Drug–light interval (h)		Survival[a] (%) Drug–light interval (h)	
	1	3	1	3
Ce6	NA[b]	100[c]	0	67
Ce6–PVP	100	40 ± 9.8	100	100
Ce6–DMSO	NA[b]	NA[b]	0	0

Each data point represents a mean of 3–5 animals.
[a] The survival of mice was expressed as the number of mice which recovered from treatment at 24 h post-treatment.
[b] Tumor necrosis could not be evaluated in animals that died due to treatment toxicity.
[c] Necrotic tissue was evaluated from the 67% animals that survived PDT.

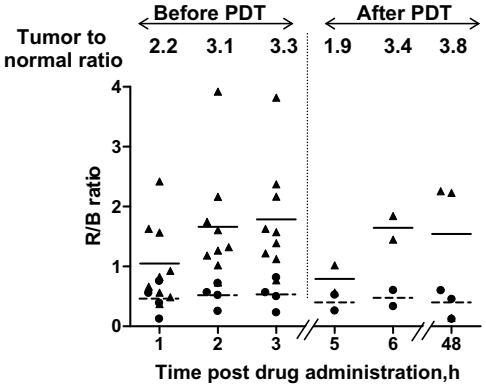

Fig. 7. Scatter plot of red-to-blue intensities in (●) normal skin and (▲) angiosarcoma lesions plotted against time from 3 patients after intravenous administration of 75% Ce6–PVP. Each circle/triangle represents different lesions or normal skin at the particular time point post-Ce6–PVP administration. Red fluorescence from the cancerous lesion was found to be higher than the surrounding normal skin. The average tumor to normal tissue ratio is indicated on top of the plot.

4. Discussion

There is a great interest in the synthesis of new generation photosensitizers with improved PDT characteristics. Chlorins are particularly strong under investigations in preclinical and clinical fluorescence diagnosis and PDT of various malignant neoplasms because of their efficient photosensitizing properties [24]. Though several methods have been proposed to enhance the efficacy of Ce6, there are still no effective pharmaceutical preparations and methods for parenteral formulations for clinical use. Many experiments have generated distinct evidence about the impact of PVP on the drug transporters, metabolic enzymes, and pharmacokinetics processes. Thus, the present study evaluated the effect of PVP on the delivery and photosensitizing properties of Ce6 photosensitizer in vitro as well as in the in vivo xenograft tumor model. Preliminary clinical data on the safety and efficacy of Ce6–PVP are also presented here.

Often, photosensitizers are administered in relatively high doses, which leads to nonspecific toxicity in normal cells. Thus it is of interest to evaluate the intrinsic sensitivity of normal (PMN cells) and cancerous (K562 cells) leukemia cells to PDT using Ce6 formulated with or without PVP using in vitro phototoxicity experiment that strictly controlled for light and photosensitizer exposure. In vitro Ce6–PVP mediated PDT studies demonstrated that leukemic cells were considerably more affected than PMN cells, supporting the hypothesis that Ce6–PVP accumulated preferentially in tumor cells compared to normal cells. This is extremely important for the application of PDT in cancer, since Ce6–PVP is intravenously administered and is supposed to localize and kill only the malignant cells after light irradiation. A recent in vitro investigation on cervical and esophageal cancer cell lines determined that the mechanism of Ce6–PVP (75% purity) induced cell death involves the induction of ROS via a type I mechanism which resulted in the rapid increase in lactate dehydrogenase that suggested characteristics of necrotic cell death pathway [25]. In our experiment, more apoptotic cells were observed and these contrary results may be due to differences in drug dosage, formulation, light dose/source and cell lines since work carried out by us and other groups has shown that the proportion of PDT-induced apoptosis and necrosis is dependent on the treatment parameters used.

In vivo biodistribution data indicated that the tumor uptake of Ce6 in the PVP formulation was enhanced compared to Ce6 alone. At the same time, Ce6–PVP accumula-

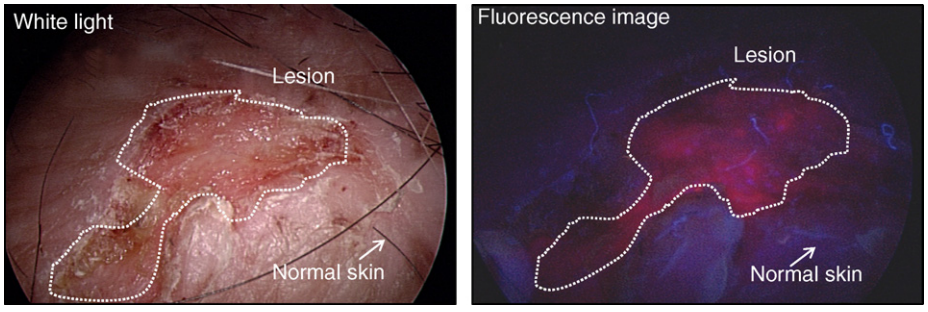

Fig. 6. White light image and its corresponding fluorescence image of angiosarcoma lesion and the surrounding normal skin at 3 h post-intravenous administration of 75% Ce6–PVP. The red fluorescence excited by the Karl Storz endoscopy system revealed the margins of the cancerous lesion.

tion in the skin was also higher than Ce6 suggesting that Ce6–PVP has the potential for skin photosensitivity in mice due to their relatively thin skin. However, this may not be a significant problem for human skin since human skin is considerably thicker than mice skin [26]. It was further confirmed that Ce6–PVP had preferential tumor accumulation in comparison with all normal tissues, with tumor to normal tissue ratio ranging from 1.4 to 25 (Table 1). The small and large intestines showed the highest fluorescence, as they are the main routes for drug elimination from the body. Not surprisingly, Ce6 delivered using DMSO showed 6-fold enhancement of Ce6 accumulation in tumor, muscle and skin compared to Ce6 alone or Ce6–PVP. This was mainly due to the membrane penetrant-carrier properties of DMSO. However, the decay rate constant of Ce6–DMSO was found to be greater than the decay rate constant of Ce6 and Ce6–PVP in tumor. This resulted in rapid elimination of Ce6–DMSO from the tumor tissues that could limit its therapeutic effect. Furthermore, it was an indication that the penetration effect provided by DMSO was irreversible in tumor and even in normal cells. Moreover, the enhanced uptake was indiscriminate and also accumulating in normal organs. This effect was clearly seen in our in vivo study.

The phototoxicity of Ce6, Ce6–PVP and Ce6–DMSO was examined in vivo using human bladder tumor-bearing mice. Ce6–PVP was found to cause greater tumor necrosis at 1 h compared to 3 h drug–light interval after exposure to 100 J/cm^2 delivered at 85 mW/cm^2 as a single fraction without causing any side effects to the mice at post-treatment. However, administration of Ce6 alone or Ce6–DMSO mediated PDT resulted in severe side effects (paralysis and death) at post-PDT. This phenomenon of acute toxicity in animals with other modes of PDT had been previously reported [27]. Adverse side effects are mainly due to PDT induced damage to normal organs [28]. This could be due to the increased solubility of Ce6 by DMSO and thus the increased uptake of Ce6–DMSO in normal tissue (Fig. 3) which resulted in acute toxicity due to irradiation to the surrounding normal tissue [15]. Furthermore, many studies have reported adverse results with respect to DMSO effects on metabolism and toxicity of other xenobiotics. It is known that DMSO is not a biologically inert compound and combinations of DMSO with other toxic agents could constitute its greatest toxic potential [29]. Therefore, the interaction of DMSO with Ce6 suggests a serious toxicological implication that needs to be taken into consideration when giving parenteral administration. Post-PDT toxicity observed for Ce6 alone can be attributed to the fact that the chlorins are extremely potent photosensitizer. One known chlorin-based photosensitizer that was reported to have acute PDT toxicity effect is *m*-tetrahydroxyphenylchlorin [30]. The data therefore suggest that using a formulation with PVP, a significant reduction in the post-PDT systemic toxicity of Ce6 can be achieved. Because of this reduced toxicity, higher doses of Ce6–PVP than that of the parent drug can be used in PDT, allowing the treatment to be potentially repeated many times to improve efficacy without any adverse effects. However, it is important to note that PDT performed to date only used a single dose of Ce6 (e.g., 5 mg/kg). A smaller dose of Ce6 may preclude PDT related toxicity in the animals, and this warrants further studies.

The decrease in the constant decay rate of Ce6–PVP in tumor and muscle compared to Ce6 and Ce6–DMSO could also reflect the possibility that PVP may have a retention effect on the uptake of Ce6. At the moment, we hypothesize that the major therapeutic effect of Ce6–PVP observed in our study was likely to have been the result of the traditional role of PVP as a plasma expander [31]. As with any effective plasma volume expander, PVP decreases the viscosity of blood by hemodilution and thus may dilute the active Ce6 in the circulation. Interestingly, PVP has also been reported to localize in malignant tumors [32] and remained mainly in blood with no specific normal tissue distribution [33]. Furthermore, the administration of PVP was found to cause significant decreases in the plasma concentrations of total cholesterol, phospholipid and triglyceride concentrations in normal rats and hyperlipidemic human subjects [34,35]. Therefore, another hypothesis that PVP has a biological effect on the in vivo transport of Ce6 seems to be an appealing one.

The employment of fluorescence stimulation of various photosensitizing drugs and detection of identified fluorescence signals from precancerous and cancerous tissue has found its wide usage in the clinic [3]. In terms of tumor imaging, we have shown that Ce6–PVP induced fluorescence can be used as a marker in which diagnostic assumptions can be reliably based and formulated. Based on ROC analysis, Ce6–PVP induced fluorescence was found to yield high sensitivity and specificity in demarcating tumor from normal peritumoral muscle of the xenograft model compared to Ce6 alone and Ce6–DMSO. These data signify that fluorescence imaging using Ce6–PVP could be clinically relevant for determining the location of invisible cancerous lesions/tissue. In the clinical study, Ce6–PVP induced fluorescence in angiosarcoma lesions reached a peak at about 3 h post-drug administration. It was noted that Ce6–PVP could enhance the image contrast between the diseased lesion and surrounding normal tissue in the fluorescence image. The appreciable red fluorescence emission of Ce6–PVP captured using a CCD camera system together with digital imaging, can be utilized either for a directed biopsy or for preoperative planning to demarcate tumor margins. The routine employment of such systems is being assessed in studies with other photosensitizers in various oncologic and non-oncologic applications of the skin [36]. The loss of fluorescence at 5 h could be attributed to the photobleaching effect of Ce6–PVP immediately after PDT. Interestingly, the red fluorescence recovered at 6 h post-drug administration, suggesting that the circulating Ce6–PVP in the serum seemed to be redistributed into the lesions after PDT. At 48 h, the tumor to normal tissue ratio of fluorescence was found to be similar to the ratio at

3 h post-drug administration. However, the PDT efficacy at 48 h drug–light interval might not be good due to an overall decrease in the photosensitizer level in the lesions, which may cause a decrease in tumor response due to the photosensitizer threshold that is needed for a good response. We have reported that PDT performed at 3 h drug–light interval was effective in achieving local control of the angiosarcoma lesions for up to 14 months [18]. This is in agreement with other clinical PDT protocols using another hydrophilic Ce6 derivative (Npe6), where light irradiation is performed around 3–8 h post-drug administration with minimal systemic photosensitization [37,38]. Further, this study also confirms that Ce6–PVP has a faster elimination rate in the normal human skin compared to other porphyrin-based photosensitizers [39], indicating that Ce6–PVP may not cause prolonged substantial skin photosensitization in human.

In conclusion, the studies reported herein demonstrated that Ce6 delivered using PVP has a higher sensitivity and specificity for tumors and is able to induce cell death in tumor following PDT without acute toxicity in mice compared to Ce6 alone or Ce6–DMSO. We have also shown that Ce6–PVP is safe for use in patients and have observed selective uptake in angiosarcoma lesions compared to normal skin.

Acknowledgements

We thank HAEMATO-science GmbH, Germany for providing the photosensitizers and Dr. Othmar Dill for valuable comments. W.W. Chin and P.S.P. Thong are the recipients of the Singapore Millennium Foundation scholarship.

References

[1] J. Moan, Q. Peng, An outline of the hundred-year history of PDT, Anticancer Res. 23 (5A) (2003) 3591–3600.
[2] M. Olivo, W. Chin, Perylenequinones in photodynamic therapy: cellular versus vascular response, J. Environ. Pathol. Toxicol. Oncol. 25 (1-2) (2006) 223–238.
[3] S. Andersson-Engels, C. Klinteberg, K. Svanberg, S. Svanberg, In vivo fluorescence imaging for tissue diagnostics, Phys. Med. Biol. 42 (5) (1997) 815–824.
[4] K. Komagoe, K. Tamagake, T. Katsu, The influence of aggregation of porphyrins on the efficiency of photogeneration of hydrogen peroxide in aqueous solution, Chem. Pharm. Bull. (Tokyo) 54 (7) (2006) 1004–1009.
[5] C. Tanielian, C. Schweitzer, R. Mechin, C. Wolff, Quantum yield of singlet oxygen production by monomeric and aggregated forms of hematoporphyrin derivative, Free Radic. Biol. Med. 30 (2) (2001) 208–212.
[6] M.L. Adams, A. Lavasanifar, G.S. Kwon, Amphiphilic block copolymers for drug delivery, J. Pharm. Sci. 92 (7) (2003) 1343–1355.
[7] Y.N. Konan, R. Gurny, E. Allemann, State of the art in the delivery of photosensitizers for photodynamic therapy, J. Photochem. Photobiol. B 66 (2) (2002) 89–106.
[8] C.F. van Nostrum, Polymeric micelles to deliver photosensitizers for photodynamic therapy, Adv. Drug. Deliv. Rev. 56 (1) (2004) 9–16.
[9] J.G. Shiah, Y. Sun, C.M. Peterson, R.C. Straight, J. Kopecek, Antitumor activity of *N*-(2-hydroxypropyl) methacrylamide copolymer–Mesochlorine e6 and adriamycin conjugates in combination treatments, Clin. Cancer Res. 6 (3) (2000) 1008–1015.
[10] M.R. Hamblin, J.L. Miller, I. Rizvi, B. Ortel, E.V. Maytin, T. Hasan, Pegylation of a chlorin(e6) polymer conjugate increases tumor targeting of photosensitizer, Cancer Res. 61 (19) (2001) 7155–7162.
[11] P. Westerman, T. Glanzmann, S. Andrejevic, D.R. Braichotte, M. Forrer, G.A. Wagnieres, P. Monnier, H. van den Bergh, J.P. Mach, S. Folli, Long circulating half-life and high tumor selectivity of the photosensitizer meta-tetrahydroxyphenylchlorin conjugated to polyethylene glycol in nude mice grafted with a human colon carcinoma, Int. J. Cancer 76 (6) (1998) 842–850.
[12] A.N. Lukyanov, V.P. Torchilin, Micelles from lipid derivatives of water-soluble polymers as delivery systems for poorly soluble drugs, Adv. Drug. Deliv. Rev. 56 (9) (2004) 1273–1289.
[13] Y. Kaneda, Y. Tsutsumi, Y. Yoshioka, H. Kamada, Y. Yamamoto, H. Kodaira, S. Tsunoda, T. Okamoto, Y. Mukai, H. Shibata, S. Nakagawa, T. Mayumi, The use of PVP as a polymeric carrier to improve the plasma half-life of drugs, Biomaterials 25 (16) (2004) 3259–3266.
[14] B. Ramaswamy, V. Manivasager, W.W. Chin, K.C. Soo, M. Olivo, Photodynamic diagnosis of a human nasopharyngeal carcinoma xenograft model using the novel Chlorin e6 photosensitizer Fotolon, Int. J. Oncol. 26 (6) (2005) 1501–1506.
[15] W.W. Chin, W.K. Lau, P.W. Heng, R. Bhuvaneswari, M. Olivo, Fluorescence imaging and phototoxicity effects of new formulation of chlorin e6-polyvinylpyrrolidone, J. Photochem. Photobiol. B 84 (2) (2006) 103–110.
[16] W.W. Chin, W.K. Lau, R. Bhuvaneswari, P.W. Heng, M. Olivo, Chlorin e6-polyvinylpyrrolidone as a fluorescent marker for fluorescence diagnosis of human bladder cancer implanted on the chick chorioallantoic membrane model, Cancer Lett. (2006).
[17] W.W. Chin, P.W. Heng, R. Bhuvaneswari, W.K. Lau, M. Olivo, The potential application of chlorin e6-polyvinylpyrrolidone formulation in photodynamic therapy, Photochem. Photobiol. Sci. 5 (11) (2006) 1031–1037.
[18] P.S. Thong, K.W. Ong, N.S. Goh, K.W. Kho, V. Manivasager, R. Bhuvaneswari, M. Olivo, K.C. Soo, Photodynamic-therapy-activated immune response against distant untreated tumours in recurrent angiosarcoma, Lancet Oncol. 8 (10) (2007) 950–952.
[19] H.A. Isakau, T.V. Trukhacheva, P.T. Petrov, Isolation and identification of impurities in chlorin e6, J. Pharm. Biomed. Anal. (2007).
[20] W.W. Chin, P.W. Heng, M. Olivo, Chlorin e6–polyvinylpyrrolidone mediated photosensitization is effective against human non-small cell lung carcinoma compared to small cell lung carcinoma xenografts, BMC Pharmacol. 7 (1) (2007) 15.
[21] H.A. Isakau, T.V. Trukhacheva, A.I. Zhebentyaev, P.T. Petrov, HPLC study of chlorin e6 and its molecular complex with polyvinylpyrrolidone, Biomed. Chromatogr. 21 (3) (2007) 318–325.
[22] W. Zheng, M. Olivo, K.C. Soo, The use of digitized endoscopic imaging of 5-ALA-induced PPIX fluorescence to detect and diagnose oral premalignant and malignant lesions in vivo, Int. J. Cancer. 110 (2) (2004) 295–300.
[23] D.A. Bellnier, W.R. Greco, J.C. Parsons, A.R. Oseroff, A. Kuebler, T.J. Dougherty, An assay for the quantitation of Photofrin in tissues and fluids, Photochem. Photobiol. 66 (2) (1997) 237–244.
[24] R.K. Pandey, D.A. Bellnier, K.M. Smith, T.J. Dougherty, Chlorin and porphyrin derivatives as potential photosensitizers in photodynamic therapy, Photochem. Photobiol. 53 (1) (1991) 65–72.
[25] L. Copley, P. van der Watt, K.W. Wirtz, M.I. Parker, V.D. Leaner, Photolontrade mark, a chlorin e6 derivative, triggers ROS production and light-dependent cell death via necrosis, Int. J. Biochem. Cell Biol. (2007).
[26] G.A. Simon, H.I. Maibach, Relevance of hairless mouse as an experimental model of percutaneous penetration in man, Skin Pharmacol. Appl. Skin Physiol. 11 (2) (1998) 80–86.
[27] T.J. Dougherty, Photosensitizers: therapy and detection of malignant tumors, Photochem. Photobiol. 45 (6) (1987) 879–889.

[28] F.H. van Duijnhoven, J.P. Rovers, K. Engelmann, Z. Krajina, S.F. Purkiss, F.A. Zoetmulder, T.J. Vogl, O.T. Terpstra, Photodynamic therapy with 5,10,15,20-tetrakis(*m*-hydroxyphenyl) bacteriochlorin for colorectal liver metastases is safe and feasible: results from a phase I study, Ann. Surg. Oncol. (2005).
[29] C.F. Brayton, Dimethyl sulfoxide (DMSO): a review, Cornell Vet. 76 (1) (1986) 61–90.
[30] H.B. Ris, A. Giger, V.I. Hof, D. Mettler, J.C. Stewart, U. Althaus, H.J. Altermatt, Experimental assessment of photodynamic therapy with chlorins for malignant mesothelioma, Eur. J. Cardiothorac. Surg. 12 (4) (1997) 542–548.
[31] E.A. Moffitt, Blood substitutes, Can. Anaesth. Soc. J. 22 (1) (1975) 12–19.
[32] S.W. Young, H.H. Muller, B. Marincek, Contrast enhancement of malignant tumors after intravenous polyvinylpyrrolidone with metallic salts as determined by computed tomography, Radiology 138 (1) (1981) 97–105.
[33] H. Kodaira, Y. Tsutsumi, Y. Yoshioka, H. Kamada, Y. Kaneda, Y. Yamamoto, S.-i. Tsunoda, T. Okamoto, Y. Mukai, H. Shibata, S. Nakagawa, T. Mayumi, The targeting of anionized polyvinylpyrrolidone to the renal system, Biomaterials 25 (18) (2004) 4309–4315.
[34] J.C. Allen, J.H. Baxter, H.C. Goodman, Effects of dextran, polyvinylpyrrolidone and gamma globulin on the hyperlipidemia of experimental nephrosis, J. Clin. Invest. 40 (1961) 499–508.
[35] S.S. Sanbar, G. Smet, Hypolipidemic effect of polyvinylpyrrolidone in man, Circulation 38 (4) (1968) 771–776.
[36] R.M. Szeimies, M. Landthaler, Photodynamic therapy and fluorescence diagnosis of skin cancers, Recent Results Cancer Res. 160 (2002) 240–245.
[37] A.L. Chan, M. Juarez, R. Allen, W. Volz, T. Albertson, Pharmacokinetics and clinical effects of mono-L-aspartyl chlorin e6 (NPe6) photodynamic therapy in adult patients with primary or secondary cancer of the skin and mucosal surfaces, Photodermatol. Photoimmunol. Photomed. 21 (2) (2005) 72–78.
[38] S.W. Taber, V.H. Fingar, C.T. Coots, T.J. Wieman, Photodynamic therapy using mono-L-aspartyl chlorin e6 (Npe6) for the treatment of cutaneous disease: a Phase I clinical study, Clin. Cancer Res. 4 (11) (1998) 2741–2746.
[39] W.G. Roberts, K.M. Smith, J.L. McCullough, M.W. Berns, Skin photosensitivity and photodestruction of several potential photodynamic sensitizers, Photochem. Photobiol. 49 (4) (1989) 431–438.